Chapter 1

A REVIEW OF DELBRÜCK SCATTERING

1.1. Delbrück scattering as a non-linear QED phenomenon

Quantum electrodynamics (*QED*) is the quantum field theory of electrodynamics describing all phenomena involving electromagnetic interactions. The impressive predictive power and the remarkable agreement of all the predictions of *QED* with experiments remain an inspiration for theories of other interactions too. Basically constructed from Maxwell's classical theory of electrodynamics incorporating relativistic quantum mechanics, *QED* generally describes the electromagnetic scattering amplitudes as a perturbative expansion in powers of the fine structure constant α (= $e^2/\hbar c \approx 1/137$). *QED* can predict several reactions such as pair production and annihilation which have no counterpart in classical physics. More interestingly *QED* admits nonlinear processes like scattering of photons by photons [1]. As Maxwell's electrodynamics is a linear theory obeying the principle of superposition, the scattering of a photon by a photon or by an electrostatic field in empty space is simply not possible in it. The root of the non-classical nonlinear effects in *QED* is vacuum polarization, a consequence of *QED*.

Classically, vacuum constitutes a trivial nothingness but in *QED* vacuum has certain rich structure. Due to fluctuation of an external fermion field, inserted into a vacuum, virtual particle-antiparticle pairs are created. The pairs act as dipoles and so the vacuum becomes polarized. The polarizability of vacuum is in some ways analogous to that of an inhomogeneous dielectric. The vacuum polarization is dominated by the lightest charged particles (electrons) and the separation distance between the electron pairs cannot exceed the Compton wavelength of electron due to the uncertainty principle. The phenomenon of vacuum polarization leads to a modification of Coulomb's 1/r law at distances smaller than the electron's Compton wavelength leading to a phenomenological departure from the linearity of Maxwell's equations.

The vacuum polarization has several implications on atomic spectroscopy as well as on scattering processes which have no classical counterparts. As mentioned already, in *QED* a photon can give rise to an electron-positron pair in the presence of a strong enough electric field out of vacuum, so possibilities are opened up for new non-classical "scattering channels" where outgoing states are different than the elementary one. For instance the virtual charged particle pair so created can interact with another photon thereby leading to the light scattering by light. On the other hand if the virtual charged particle pair interacts with the external field, the so called *Delbrück* scattering [2] may occur in which subsequent annihilation of the virtual pair gives the overall effect of the scattering of a photon by an external potential. Other nonlinear processes of *QED* include photon splitting (the primary photon is split into two photons by interaction with the static Coulomb field of the target nuclei) [1, 3-5, 79], Coalescence of photons [5], Multiphoton Compton scattering [6], Unruh effect [7] and so on.

Among the different nonlinear scattering events admissible in *QED*, scattering of light by light has drawn particular interest for long time as the phenomenon presumably is an extreme form of simple vacuum polarization but till now a direct experimental detection of the phenomenon with real photon has not been possible because of the extremely small cross section and the difficulty of producing dense targets in laboratory. The elastic scattering of photon with Coulomb field of nuclei (Delbrück scattering) and splitting of photons on nuclei have been experimentally observed and investigated.

Out of all the nonlinear processes of *QED* the Delbrück scattering was the first proposed one and it is also the oldest one to be detected experimentally. In 1933 Delbrück [2] had introduced this new kind of elastic scattering of photon in order to explain an excess count of elastically scattered photons of 2.615 MeV from lead and iron in an experiment carried out by Meitner and Koster [2]. Delbrück proposed that the unaccounted for part of the elastic scattering counts could be explained by means of Dirac –sea. It was argued that the Delbrück scattering could be viewed as a kind of Rayleigh scattering by the negative- energy electrons of Dirac (positrons). Delbrück scattering has to be elastic since there are no free states into which negative-energy electrons can recoil. Delbrück's proposal was considered seriously as, by that time, Dirac's theory was already a big success after the discovery of positrons by Anderson. A few months later (in the same year) Halpern [1] had proposed photon splitting and photon-photon scattering. The relationship of these non-linear *QED* phenomena can be assessed by looking at the corresponding Feynman diagrams in Fig.1.1. Of these processes Delbrück scattering is the most investigated one as it can be precisely tested in an experiment.

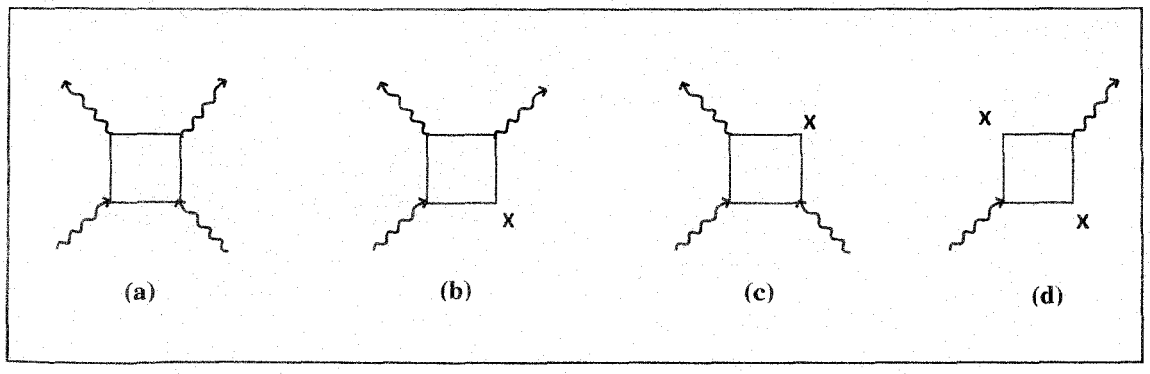

Fig.1.1. Feynman diagrams for (a) photon-photon scattering, (b) photon splitting, (c) photons coalescence and (d) Delbrück scattering. Here 'X' stands for external electromagnetic field.

Being an electromagnetic reaction Delbrück scattering should be, in principle, fully explained by *QED*. But even after seventy-five years of its discovery, there is no general theoretical solution of Delbrück scattering problem for arbitrary photon-energies

3and scattering-angles and it remains a challenge to the physics-community, although a fair understanding of the phenomenon has been achieved so far. An early general review on the topic was due to Papatzacos and Mork [8] in 1975. Subsequent review works by Milstein and Schumacher [9] in 1994 and by Schumacher [10] in 1999 cover the most of the important activities on the topic both in theory and in experimental front till mid nineties. Taking the progress of this field over the last decade (for instance [11-17]) into consideration, a brief description of the theoretical frameworks of Delbrück scattering and a summary of the current status of experimental detection of the effect would be presented in this chapter.

1.2. Theoretical aspects of Delbrück scattering

In Delbrück scattering an incident photon is assumed to get converted into a pair of electron and positron in the Coulomb field of the scattering nucleus, and then interact with the nucleus via virtual photons and again recombine to form the final photon having the same energy as that of the incident photon. The external field, by which the virtual charged particle pair is deflected, is provided by the Coulomb field of the nucleus and it must remain static for the scattering to be elastic. When the incident photon energy is very small compared to the rest mass of the nucleus, the nuclear recoil is negligible and the Coulomb field of the nucleus can be assumed to be static.

Although the first breakthrough in both the theoretical as well as experimental investigation of Delbrück scattering came in the early seventies, several theorists and experimentalists made numerous attempts to investigate the effect right after its discovery in 1933. The contributions of those early workers [18-30] to this field greatly helped in the general understanding and continuous development of the subject and are well documented in [8]. In the present review the discussions are limited to the results which are relevant as on today without emphasizing on the chronological development of the subject.

Certain general ideas about the nature of Delbrück scattering were obtained on the basis of simple physical arguments. For example, a rough estimate of the Delbrück scattering cross section can be made through the following simple approach. The requirement of gauge invariance demands that as $\omega \to 0$ (we choose the units in which $\hbar = c = 1$ unless otherwise stated and therefore the energy of incident photon = ω) the scattering amplitude should contain products of the 4-momenta of the initial photon and the final photon. The scattering involves second and higher order *QED* processes and is due to external Coulomb field of the nucleus with charge Ze (Z being the atomic number of the scattering atom and e the electronic charge). So at the zero-th level the scattering amplitude is expected to include external field in second order. Therefore, one may conclude that for small photon energies ($\omega << m$) the scattering cross section would be

$$d\sigma \sim (Z\alpha)^4 r_e^2 (\omega/m)^4 d\Omega, \tag{1.1}$$

where m is the rest mass of an electron and r_e is the classical electron radius. Some information about the scattering cross section can be extracted by the applications of the optical theorem and dispersion relation. It is well known that the absorption of photons is inevitably related to a corresponding scattering process. The photoabsorption by the electrons of an atom is connected to Rayleigh scattering, the photoabsorption by the nucleus is connected to nuclear resonance scattering and the photoabsorption through e^+-e^- pair production in the Coulomb field of the nucleus is related to Delbrück scattering. Thus the forward Delbrück scattering amplitude can be estimated from the pair production cross section exploiting the optical theorem and dispersion relation [29]. At photon energy ω the imaginary part of forward elastic Delbrück scattering amplitudes $A^D(\omega, \theta = 0)$ is related to the total pair-production cross sections $\sigma^{PP}(\omega)$ through the optical theorem

$$\mathrm{Im}\, A^D(\omega,0) = \frac{\omega}{4\pi}\sigma^{PP}(\omega). \tag{1.2}$$

The real part of the scattering amplitude can be determined from the imaginary part through dispersion relation

$$\mathrm{Re}\,A^{D}(\omega,0)=\frac{\omega^{2}}{2\pi^{2}}\int_{2m}^{\infty}d\omega'\frac{\sigma^{PP}(\omega')}{(\omega'^{2}-\omega^{2})}. \tag{1.3}$$

The expression of cross section for pair production σ^{PP} by a photon in the field of a nucleus can be estimated using Born approximation calculations and then inserting that into eqns.(1.2) and (1.3) one can obtain in the ultra relativistic limit ($\omega >> m$) [30]

$$\mathrm{Im}\,A^{D}(\omega,0)=\frac{7}{9\pi}(Z\alpha)^{2}r_{e}\frac{\omega}{m}\left(\log\frac{2\omega}{m}-\frac{109}{42}\right) \tag{1.4}$$

$$\mathrm{Re}\,A^{D}(\omega,0)=(Z\alpha)^{2}r_{e}\left(\frac{7}{18}\frac{\omega}{m}-\frac{9}{4}\right) \tag{1.5}$$

Note that the real part of the magnitude does not contain any large logarithmic term unlike the expression of the imaginary part. The sum of the squares gives the total forward cross section for the Delbrück scattering in the limit $\omega >> 2m$

$$\frac{d\sigma}{d\Omega}=\frac{49}{81\pi^{2}}(Z\alpha)^{4}r_{e}^{2}\left(\frac{\omega}{m}\right)^{2}\left[\log^{2}\left(\frac{2\omega}{m}\right)+\frac{\pi^{2}}{4}\right]. \tag{1.6}$$

In the non-relativistic case ($\omega << m$)

$$\mathrm{Im}\,A^{D}(\omega,0)=0\,, \tag{1.7}$$

$$\mathrm{Re}\,A^{D}(\omega,0)=\frac{73}{2304}(Z\alpha)^{2}r_{e}\left(\frac{\omega}{m}\right)^{2} \tag{1.8}$$

and near pair production threshold ($\omega \sim 2m$)

$$\mathrm{Im}\,A^{D}(\omega,0)=\tfrac{1}{3}(Z\alpha)^{2}r_{e}(1-2m/\omega)^{3}. \tag{1.9}$$

Rohrlich and Gluckstern [30] also evaluated the corresponding Feynman graphs and obtained the similar results. The above expressions for forward scattering are very useful in the sense that they offer a first check to any new result derived in a rigorous manner.

The modern approaches of computing Delbrück scattering cross section are based on Feynman propagator method. Essentially the scattering amplitudes are obtained by

summing the Feynman diagrams with an arbitrary number of photons exchanged with a Coulomb center. Feynman diagrams representing Delbrück scattering are shown in Fig.1.2 where only the graphs having even number of vertices are considered as Fury's theorem [31] forbids closed fermion loops with an odd number of vertices. The first

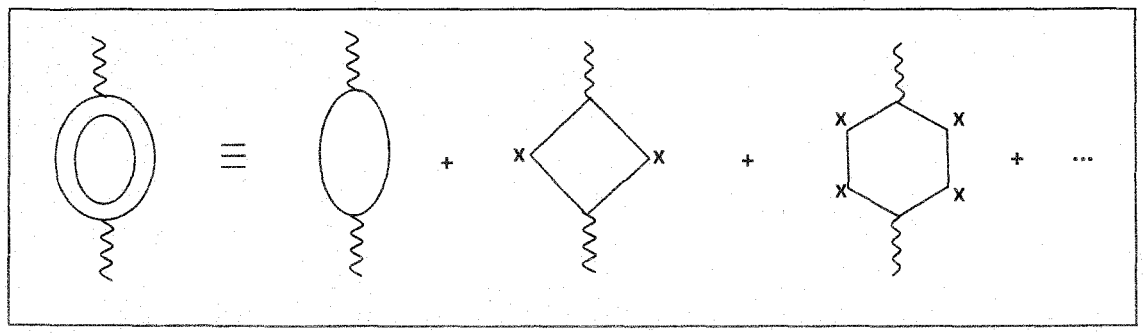

Fig.1.2. Feynman diagrams for Delbrück scattering. Here 'X' symbolizes the interaction of the virtual particles with the Coulomb field of the nucleus via a virtual photon.

diagram of the schematic expansion shown in the right hand side of Fig.1.2 does not contribute to the scattering amplitude, since it represents the self energy of a free photon. The second diagram of the series in Fig.1.2, in which two virtual photons are exchanged

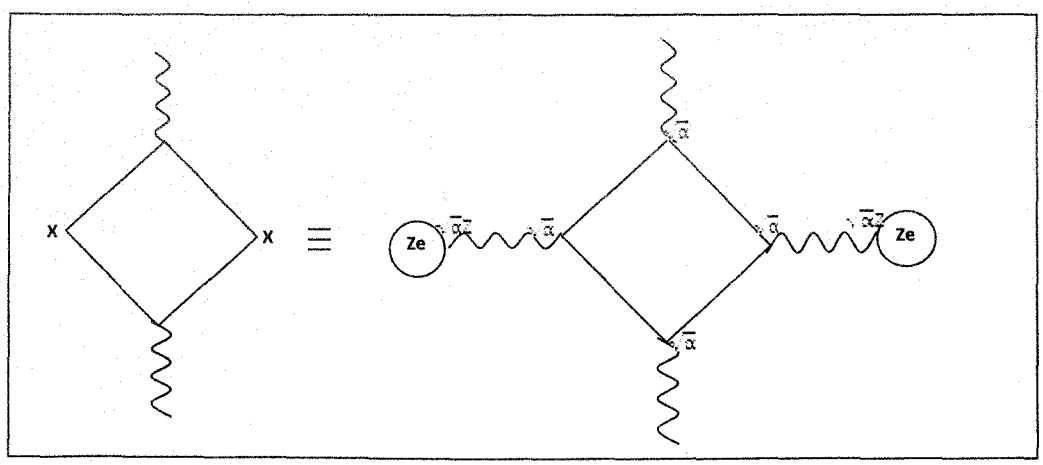

Fig.1.3. This figure illustrates that the lowest order Delbrück amplitude is of order $\alpha(\alpha Z)^2$.

with the nucleus, represents the lowest order Delbrück scattering and is of order $\alpha(\alpha Z)^2$. It is straightforward to estimate the order of each term in Fig.1.2 as can be seen from an illustration in Fig.1.3 where the lowest order reaction is considered. The next higher-order terms will be of order $\alpha(\alpha Z)^4$, $\alpha(\alpha Z)^6$ and so on.

The second term of Fig.1.2 representing the lowest-order scattering process, actually consists of three permutations which are depicted in Fig.1.4. Similarly, all the possible permutations of the higher order graphs should also be taken into account when one intends to evaluate the higher order terms. The scattering amplitudes corresponding to the four-cornered loops, as given in Fig.1.4, are related to the rank-four vacuum polarization tensor $\Pi_{\mu\nu\lambda\sigma}$. Due to vacuum polarization the free photon propagator is modified since the covariant photon can virtually disintegrate into an electron-positron pair for a certain fraction of time which is quantified by vacuum polarization tensor. Amplitudes of other related non-linear effects of *QED* like photon-photon scattering, photon-splitting etc. are also calculated from this general tensor. In case of Delbrück scattering, the vacuum polarization tensor $\Pi_{\mu\nu\lambda\sigma}$ specializes to $\Pi_{\mu\nu 44}$ as there is no energy transfer between the photon and the nucleus.

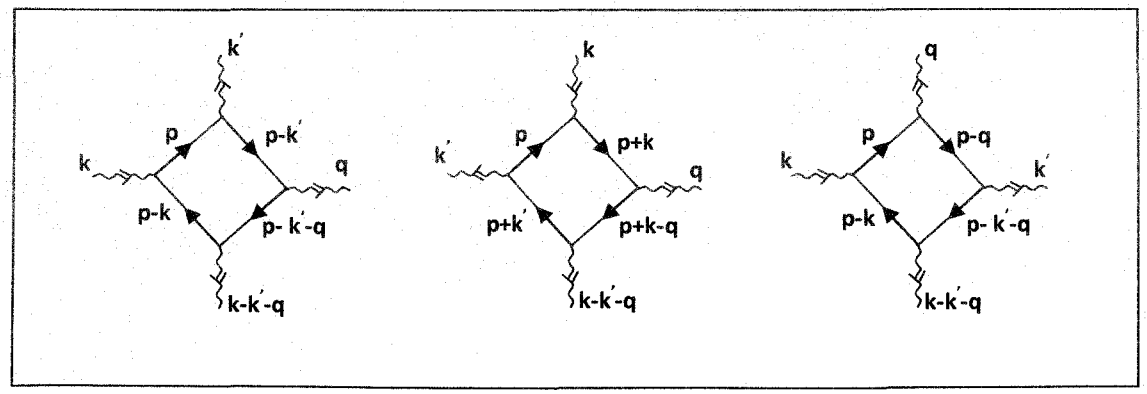

Fig.1.4.The three permutations of Feynman diagram for the lowest order Delbrück scattering.

The vacuum polarization tensor $\Pi_{\mu\nu\lambda\sigma}$ is defined through Green function ($G_{\mu\nu\lambda\sigma}$) of the Dirac equation in the external Coulomb field of nucleus as

$$\Pi_{\mu\nu\lambda\sigma} = G_{\mu\nu\lambda\sigma}(k,k',q) - G_{\mu\nu\lambda\sigma}(0,0,0) \tag{1.10}$$

where

$$G_{\mu\nu\lambda\sigma}(k,k',q) = T_{\mu\nu\lambda\sigma}(k,k',q) + T_{\nu\mu\lambda\sigma}(-k',-k,q) + T_{\mu\lambda\nu\sigma}(k,q,k') \tag{1.11}$$

and

$$T_{\mu\nu\lambda\sigma}(k,k',q) = \int d^4p\ Tr\left(\gamma_\mu \frac{1}{i\gamma.p+m}\gamma_\nu \frac{1}{i\gamma.(p-k')+m}\gamma_\lambda \frac{1}{i\gamma.(p-k'-q)+m}\gamma_\sigma \frac{1}{i\gamma.(p-k)+m}\right) \tag{1.12}$$

.

Here k and k' are four momenta of the incident and scattered photon respectively, p and q are the variable four momenta of the virtual loop-particle and the virtual photon respectively (see Fig.1.4). The term $G_{\mu\nu\lambda\sigma}$ consists of three $T_{\mu\nu\lambda\sigma}$ terms (see eqn.(1.11)) corresponding to the three diagrams of Fig.1.4. Although each of these $T_{\mu\nu\lambda\sigma}$ terms diverges logarithmically for large values of p, the divergences cancel in $G_{\mu\nu\lambda\sigma}$. However, $G_{\mu\nu\lambda\sigma}$ is not gauge-invariant. The gauge-invariant vacuum polarization tensor $\Pi_{\mu\nu\lambda\sigma}$ is obtained in eqn.(1.10) by a subtraction procedure. Then one can write the lowest-order Delbrück scattering amplitude as

$$A^D = -i(Z\alpha)^2 r_e \frac{m}{8\pi^5}\int \frac{d^3q}{\vec{q}^{\,2}} \frac{\varepsilon^\mu(k)\varepsilon^\nu(k')}{(\vec{q}-\vec{\Delta})^2}\Pi_{\mu\nu 44}(k,k',q) \tag{1.13}$$

where $\varepsilon^\mu(k)$ and $\varepsilon^\nu(k')$ are the linear polarization vectors of the incoming and outgoing photons respectively, and $\vec{\Delta}$ is the momentum transfer , $\vec{\Delta} = \vec{k} - \vec{k}'$.

The Delbrück scattering amplitude A^D as defined through eqns.(1.10-1.13) is, in principle, calculable for arbitrary photon-energy and scattering angle. However, the procedure is so tedious and complicated that an exact solution useful for practical purposes has not been realized as yet.

The lowest order Delbrück scattering amplitude, in which only two photons are considered to be exchanged with the nucleus, is of order $\alpha(Z\alpha)^2$. If, more generally, 2n photons are exchanged with the nucleus, then the A^D is of order $\alpha(Z\alpha)^{2n}$ for n=1, 2, 3. For heavy nuclei, higher powers of $Z\alpha$ are not negligible, as such all the higher order Feynman diagrams should also be summed up in order to make accurate prediction of A^D. In other words, effects of multi-photon exchange should be included in the lowest order results. Such correction to the lowest order amplitude is called Coulomb correction.

Alternatively the Delbrück scattering scenario can be described through transition (T) matrix and using the quasiclassical Green function of the Dirac equation in a Coulomb field of nucleus. The basic methodology of treating the problem is to solve the Dirac equation in presence of external Coulomb field in terms of Green function and then construct the transition amplitude. If an incoming photon of four-momenta k (=ω, **k**) and polarization four-vector $\varepsilon^{\mu}(k)$ produce a pair of virtual electron-positron pair at the point **x** which (the virtual pair) annihilate to an outgoing photon of four-momenta k' (=ω, **k**') and polarization four-vector $\varepsilon^{\nu}(k)$ at the point **x**', then the corresponding transition amplitude is

$$A^D = 2i\alpha \int d^3\mathbf{x}\, d^3\mathbf{x}' \exp[i(\mathbf{k}.\mathbf{x} - \mathbf{k}'.\mathbf{x}')] \times \int dz_1\, dz_2\, \delta(\omega - z_1 + z_2) Tr\left[\gamma_\nu \varepsilon^\nu(k) G(\mathbf{x},\mathbf{x}' \mid z_2)\left[\gamma_\mu \varepsilon^\mu(k')\right]^* G(\mathbf{x}',\mathbf{x} \mid z_1)\right] \quad (1.14)$$

Owing to the complexity of the calculations, all the theories of Delbrück scattering developed so far have their own ranges of validity. We mention below the predictions generally valid at three regions; (1) high energies and small angles, (2)

intermediate energies and moderately large angles and (3) low energies and all angles. The detail of validity and correctness of these theoretical predictions are elaborated in the sections containing experimental results.

1.2.1. Theories for high energies and small angles

The theory for this regime based on the quasiclassical treatment was developed by Milstein *et al.* [32, 33], which yields A^D correct to all orders in $Z\alpha$ at high energies and small angles. Starting from eqn.(1.14) and arguing that in the complex plane z, of which the real axis varies from -∞ to +∞, the Green function $G(\mathbf{x},\mathbf{x}'|z)$ has simple poles in the interval –m to + m corresponding to discrete spectrum and has the cuts from -∞ to –m and from m to ∞ corresponding to the continuous spectrum, they have tactfully deformed the countours of the integration. It can be noted that for $\omega >> m$ the contribution of the discrete spectrum can be ignored. Writing the δ-function of eqn. (1.14) as

$$\delta(\omega - z_1 + z_2) = \frac{i}{2\pi}\left(\frac{1}{\omega - z_1 + z_2 + i0} - \frac{1}{\omega - z_1 + z_2 - i0}\right), \tag{1.15}$$

and using the analytic properties of $G(\mathbf{x},\mathbf{x}'|z)$ [34], the A^D for $\omega >> m$ can be written as

$$\begin{aligned} A^D = \frac{\alpha}{\pi} \int d^3\mathbf{x}\, d^3\mathbf{x}' \exp[i(\mathbf{k}.\mathbf{x} - \mathbf{k}'.\mathbf{x}')] \int_m^\infty \int_m^\infty dz_1\, dz_2 \\ \times Tr\left(\frac{\gamma_\nu \varepsilon^\nu(k)\,\delta G(\mathbf{x},\mathbf{x}'|-z_2)(\gamma_\mu \varepsilon^\mu(k'))^* G(\mathbf{x}',\mathbf{x}|z_1)}{\omega - z_1 - z_2 + i0} \right. \\ \left. - \frac{\gamma_\nu \varepsilon^\nu(k)\,\delta G(\mathbf{x},\mathbf{x}'|z_2)(\gamma_\mu \varepsilon^\mu(k'))^* G(\mathbf{x}',\mathbf{x}|-z_1)}{\omega + z_1 + z_2 - i0} \right) \end{aligned} \tag{1.16}$$

where $\delta G(\varepsilon) = G(\varepsilon + i0) - G(\varepsilon - i0)$ is the discontinuity of the Green function. Arguing in terms of basic concepts Milstein *et al.* have shown that the angular momentum l of the particles created in the loop is $l \sim \omega/\Delta >> 1$ [9] and that the dominant contribution to the amplitude is made within the region $m^2/\omega << \Delta << \omega$. Then, they make quasi-classical

approximation by replacing the summation over l in the expansion of δG by an integration. The asymptotic forms of amplitudes for $\omega >> \Delta >> m$ are

$$A_{++}^{D} \approx \frac{4i}{3}\frac{2\alpha\omega}{\Delta^2}\left(1-\frac{2\pi Z\alpha}{\sinh(2\pi Z\alpha)}\left[1-2Z^2\alpha^2\right]\right) \tag{1.17}$$

$$A_{+-}^{D} \approx \frac{4i}{3}\frac{2\alpha\omega}{\Delta^2}Z^2\alpha^2\left[1-(Z\alpha)\,\mathrm{Im}\,\psi'(1-iZ\alpha)\right] \tag{1.18}$$

where $A_{\parallel}^{D} = (A_{++}^{D} + A_{+-}^{D})$, $A_{\perp}^{D} = (A_{++}^{D} - A_{+-}^{D})$, the subscript +/- denote the polarization state and ψ is the logarithmic derivative of the gamma function($\psi(x) = d\{\ln\Gamma(x)\}/dx$) and $\psi' = d\psi/dx$. The forward scattering amplitude (eqn.(1.4)) is reproduced naturally in this approach.

The first theoretical calculations of Delbrück scattering based on Feynman *QED* and valid at high photon energies and small scattering angles were due to Cheng and Wu [35-42]. Initially they obtained, working in impact factor approximation which is valid in the limit of high-energy, results [35, 36] for the lowest order Delbrück amplitude in the two different regions of momentum transfer, namely $(m^2/\omega << \Delta << m)$ and $(m << \Delta << \omega)$. In their subsequent works [37-42] Cheng and Wu, considered the effects of multiphoton exchange (Coulomb corrections). In impact factor approximation the pair of high energy particles created "see" the static Coulomb potential Lorentz contracted into a thin slab. Then, they apply non-covariant perturbation theory to this physical picture to obtain Coulomb corrected scattering amplitude [38-39]. Following this method they calculated A^{D} close to the forward direction $(\Delta << m)$ correct to all orders in $Z\alpha$ but only to the lowest order in α [41]

$$A_{\perp\parallel}^{D} \sim 4i\alpha(Z\alpha)^2\frac{\omega}{m^2}\left[\frac{7}{9}\left\{\ln\left(\frac{2\omega}{m}\right)-\frac{109}{42}-\frac{1}{2}i\pi+\gamma+\mathrm{Re}\,\psi(1+iZ\alpha)\right\} + 4\int_1^{\infty}dx\int_0^1 dy(1-y^2)^{-\frac{1}{2}}\right.$$
$$\left.\times\int_0^1 d\beta\left\{y+ixm^2/[\beta(1-\beta)\Delta\omega]\right\}^{-1}\left\{(2-y^2)[-\tfrac{1}{2}x^{-2}+x^{-4}\beta(1-\beta)(x^2-2x+2)]\mp y^2\beta(1-\beta)x^{-4}\right\}\right] \tag{1.19}$$

where –(+) is used when the photon is linearly polarized perpendicular (parallel) to the scattering plane , ψ is defined in eqn.(1.18), x, y and β are independent variables and γ is Euler's constant, numerically equal to 0.57722. In [41], they have also shown that their procedure could reproduce the forward scattering amplitude given by Rohrlich and Gluckstern (eqns.1.4 and 1.5). For large momentum transfer $(\omega >> \Delta >> m)$, the fourfold integration involving the Feynman parameters can be done analytically and the amplitudes are given by [42]

$$A^{D}_{\perp,\parallel} \sim -i\frac{e^4 Z\omega}{(2\pi)^2\Delta^2}\left[-\frac{2}{3}\frac{(1\mp 3Z^2\alpha^2)}{Z\alpha}+\frac{4\pi}{3}\frac{(1-2Z^2\alpha^2)}{\sinh(2\pi Z\alpha)}\mp 2Z^2\alpha^2\,\mathrm{Im}\,\psi'(1-iZ\alpha)\right] \qquad (1.20)$$

whereas, in the limit $\Delta >> m^2/\omega$ the amplitudes are calculated numerically from the fourfold integration [42]

$$A^{D}_{\perp,\parallel} = -4i\frac{\omega}{m^2}\alpha(Z\alpha)^2\frac{Sinh(\pi Z\alpha)}{\pi Z\alpha}\int_0^1 dx\int_0^1 d\sigma\int_0^1 dz\int_0^{1/2} dz'\cos\left\{Z\alpha\ln\frac{1-z'}{z'}\right\} \times\left[f(x,\sigma,z,z';\Delta)+g_{\parallel,\perp}(x,z)h(x,\sigma,z,z';\Delta)\right] \qquad (1.21)$$

In eqn. (1.21), f and h are rational functions of their arguments as given by Cheng and Wu [42] and $g_{\parallel}=1-8z(1-z)x(1-x)$, $g_{\perp}=1$.

The high-energy and small-angle predictions based on the above two approaches [41, 42] and [32, 33] yield the similar results and are in fair agreement with experiments [69, 11].

Some simple analytic expressions for high-energy small-angle Delbrück scattering amplitudes have also been reported [13, 43]. In [13] results have been obtained for the momentum transfer Δ<< m in the frame of the quasiclassical operator method and it is the generalization of the method developed by the authors for consideration of the

Landau-Pomeranchuk-Migdal effect [44], whereas in [43] semiclassical Green's function of the Dirac equation in the Coulomb field has been used to find the similar result. These amplitudes agree with those obtained in earlier calculations, but the structure of the expressions is much simpler than that of previously known representations, which makes numerical calculations much easier.

1.2.2. Theories for intermediate energies and moderately large angles

This regime has so far been found to be difficult to study analytically. So, simple expressions of Delbrück amplitude are not available in this region. Milstein and Shaisultanov [45] estimated Delbrück scattering amplitude based on the relativistic electron green function in a Coulomb field [34] at intermediate energies (50-100 MeV) and valid at moderately large angles. The amplitude is calculated exactly in Zα at $\omega >> m$ and $\theta \sim 1$ but neglecting the electron mass as compared to ω and Δ and the expressions obtained are quite complex [45, 46]. An interesting feature predicted for this energy range is that the Delbrück scattering amplitude exhibits scaling behavior in the form $f(\theta)/\omega$, where $\sin(\theta/2) = \Delta/2\omega$. A detail investigation of the scaling behavior of Delbrück scattering has been separately described in chapter 4.

1.2.3. Theories for low energies and all angles

Papatzacos and Mork [49], using conventional Feynman techniques and gauge invariance, obtained expressions for real and imaginary parts of Delbrück amplitude in the lowest order Born approximation. Following the approach described in eqns.(1.10-1.13) they obtained results, which could reproduce not only the expressions of forward scattering amplitudes (eqns.1.4 and 1.5) given by Rohrlich and Gluckstern [30] but also the low-energy ($\omega << m$) results (eqns.1.22-1.23) of Costantini [5].

$$A_{++}^{D} = A_{--}^{D} = (Z\alpha)^2 r_e \frac{73}{2304}\left(\frac{\omega}{m}\right)^2 \cos^2\frac{\theta}{2}, \tag{1.22}$$

$$A_{+-}^{D} = A_{-+}^{D} = (Z\alpha)^2 r_e \frac{5}{256}\left(\frac{\omega}{m}\right)^2 \sin^2\frac{\theta}{2}. \qquad (1.23)$$

In [49], numerical results for Delbrück scattering amplitude at photon energies 1.33, 7.9, 9.0, 10.83, 15.1, and 87 MeV have been presented. As expected by the authors [49] themselves their predictions, being a lowest-order calculation, require higher order corrections (Coulomb correction). An adequate theoretical prediction of Coulomb correction for all angles in this regime has not been achieved though some numerical results have been reported by Scherdin *et al.*[50], based on their S-matrix treatment [51]. Results do exist for forward angle based on the optical theorem [52, 53] but it is not clear how to extend these to finite angles, which are amenable to experiment. Calculation of Coulomb corrections based on relativistic green function of electron but for $\omega << m$ has been reported [14]. Based on their earlier works on Delbrück scattering [25] De Tollis *et al.* made considerable progress in obtaining simpler expressions for the lowest-order Delbrück amplitudes [47, 48]. The results of De Tollis *et al.* [47] are in agreement with those of Papatzacos and Mork [49]. A major collection of numerical data for Delbrück scattering amplitude was done by Falkenberg *et al.* [54]. This was used by Hubbell and Bergstrom [55] in their comparison of the Delbrück contribution to scattering with that of other photon atom processes. The paper [55] also includes an extensive bibliography. Therefore, in the few MeV range the Delbrück amplitudes are generally treated in lowest-order Born approximation [49].

Amongst the other developments in theoretical side of the low energy regime, a new calculation by Di Piazza and Milstein [12] seems to be of experimental interest. They investigated the Delbrück scattering from a Coulomb field in the presence of a laser field by treating the Coulomb field in lowest-order Born approximation and the laser field in the exact parameters of the field having arbitrary strength, spectral content, and polarization. They found [12] that the behavior of the differential cross-section of the process, particularly the angular distribution, differs substantially from that for Delbrück scattering in a pure Coulomb field. It is reported that the cross section of the process can enhance in the presence of a laser field for realistic laser parameters.

1.3. Scattering amplitudes of other elastic scatterings

Among the nonlinear processes admissible by *QED*, Delbrück scattering is relatively easier to detect as it can be investigated experimentally by measuring the elastic scattering cross section of photons by high Z scatterers. However, one major difficulty for clear observations of the process is the interference of other elastic processes of photon-atom interactions. Note that Delbrück scattering (D) is just one of the four elastic processes of photon-atom interactions. Other processes are: Rayleigh scattering by the bound atomic electrons (R), nuclear Thomson scattering by the nucleus (T), and nuclear resonance scattering by the giant dipole resonance (N). Experimentally, it is not possible to distinguish any of the mechanisms individually. The elastic differential scattering cross-section is measured experimentally and then compared with the theoretical predictions obtained by summing coherently the amplitudes of different elastic processes as shown in eqn. (1.24).

$$\frac{d\sigma}{d\Omega} = |A|^2, \tag{1.24}$$

In (1.24), the scattering amplitude A is partitioned into a coherent sum,

$$A = A^R + A^T + A^N + A^D, \tag{1.25}$$

with R, T, N, and D denoting Rayleigh, Nuclear Thomson, Nuclear resonance, and Delbrück effects respectively. In general the partitioned amplitudes A^R, A^N, and A^D are complex, while the Thomson scattering amplitude A^T is purely real. Thus for the investigation of Delbrück scattering phenomenon one needs to have accurate prediction of other processes, namely, R, T and N. This need has encouraged several theorist and experimentalists for the last seven decades to study the elastic photon-atom interactions. Before presenting brief descriptions of R, T and N scatterings in the following sub-sections, we note that the amplitude A can be expressed either in terms of linear polarization amplitudes ($A_{\parallel}, A_{\perp}$) or circular polarization amplitudes (A_{++}, A_{+-}). The unpolarized elastic differential scattering cross-section is then given by

$$\frac{d\sigma}{d\Omega} = \frac{1}{2}\left(|A_{\parallel}|^2 + |A_{\perp}|^2 \right) = \left(|A_{++}|^2 + |A_{+-}|^2 \right)$$

$$A_{++} = \frac{1}{2}\left(A_{\parallel} + A_{\perp}\right), \quad A_{+-} = \frac{1}{2}\left(A_{\parallel} - A_{\perp}\right) \tag{1.26}$$

1.3.1. Rayleigh scattering amplitudes

Rayleigh scattering is the most dominant contributor to the elastic scattering at photon energies around 1 MeV and below although its presence is seen up to about 6 MeV. A precise prediction of Rayleigh scattering is essential for the study of Delbrück scattering in the low-energy region. The simplest way of finding Rayleigh scattering amplitude is based on the form factor approximation, which is valid when the momentum transferred to the atom by the scattered photon $\hbar\Delta << mc$, the binding energy of electron $T << mc^2$ and photon energy $\hbar\omega >> T$ [56]. Note that the constants $\hbar$ and c have been restored in this section only. The atomic form factor is defined [57] as the matrix element

$$f(\Delta, Z) = \sum_{n=1}^{Z} \left\langle \Psi_o \left| \exp(i\vec{\Delta} \cdot \vec{r}_n) \right| \Psi_o \right\rangle, \tag{1.27}$$

where Ψ_o is the ground-state wave function of the atom and $\vec{r}_n$ is the radius vector from the nucleus to the n^{th} electron. For a spherically symmetric atom the form factor can be expressed as

$$f(\Delta, Z) = 4\pi \int_0^{\infty} \rho(r) \frac{\sin(\Delta r)}{(\Delta r)} r^2 dr \tag{1.28}$$

Where $\rho(r)$ is the total charge distribution normalized such that

$$4\pi \int_0^{\infty} \rho(r)\, r^2\, dr = 1 \tag{1.29}$$

Calculations of $f(\Delta, Z)$ depend on the knowledge of the atomic wave functions. Values of atomic form factor $f(\Delta, Z)$ have been obtained in several atomic models.

Numerical methods for evaluating Rayleigh amplitudes in heavy atoms, within the framework of external field quantum electrodynamics and in a relativistic self-consistent central potential, were developed by Brown *et al.* [58-60] and Johnson and Feiock [61]. Rayleigh amplitudes were calculated by Cornille and Chapdelaine [62] for the K electrons of mercury at 2.616 MeV, using second-order perturbation theory. Following the method of Brown *et al.*, Johnson and Cheng [63] calculated the Rayleigh amplitudes for the K shells of heavy atoms (Z=30 to 82) and for low energy γ-rays (0.1-1 MeV). The second-order S-matrix method of calculating Rayleigh amplitudes was further developed by the Pittsburgh group [64-66]. Following the treatment adopted by Kissel [64] the accurate S-matrix Rayleigh amplitudes of lead (Z=82) for 12 photon energies of experimental interests (22.1-2750 keV) and 8 scattering angles (0^{o} -180^{o}) have been calculated by Kissel *et al.* [66]. It is based on numerical evaluation of the relativistic second order S-matrix element in independent particle approximation, using relativistic self consistent central field wave functions [67]. The lowest-order *QED*-diagrams representing Rayleigh scattering are shown in Fig.1.5.

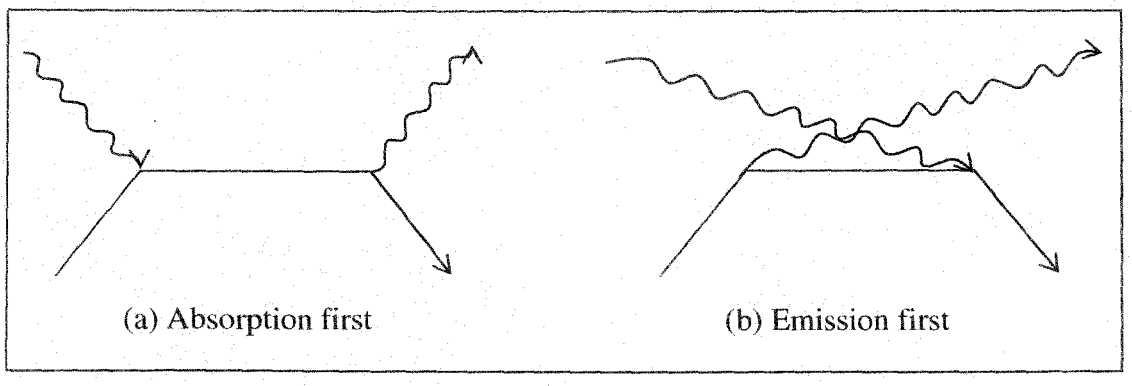

Fig.1.5.Feynman diagrams representing lowest-order Rayleigh scattering.

In S-matrix method, one is essentially evaluating

$$A_n^R = r_e\, mc^2 \sum_p \int \left[\frac{\langle n/\mathrm{A}^*/p\rangle \langle p/\mathrm{A}/n\rangle}{E_n - E_p + \hbar\omega} + \frac{\langle n/\mathrm{A}/p\rangle \langle p/\mathrm{A}^*/n\rangle}{E_n - E_p - \hbar\omega} \right] \qquad (1.30)$$

The summation and the integration are done over a complete set (bound and continuum) of intermediate states p. The operators A (A^*) represent absorption (emission) of a photon of energy $\hbar\omega$. The total Rayleigh amplitude A^R is obtained by summing over all the atomic electrons n, that is, $A^R = \sum_n A_n^R$. The S-matrix method is so far the most accurate way of obtaining the Rayleigh amplitudes.

The elastic scattering cross sections computed on the basis of form factor approximation by using different wave functions are found to vary from each other. The nonrelativistic Hartree-Fock form factors [68] provide a better prediction than the relativistic Dirac-Hartree-Fock-Slater (DHFS) form factors [69] for heavy atoms. When compared with the S-matrix Rayleigh amplitudes the form factor amplitudes calculated using DHFS wave functions are found to differ by small amounts for lighter elements (for example, 0.5 % and 0.1 % for K and L shells respectively of aluminum) but the differences are large for heavy atoms (for example, 20 %, 5 % and 2 % for K, L and M shells respectively of lead).

The numerical accuracy of S-matrix Rayleigh amplitudes are better than 1 % and the overall the agreement between experiment and theoretical prediction based on S-matrix Rayleigh amplitudes is within 3%. In spite of being the best available method, the direct numerical S-matrix method is not useful in calculating the Rayleigh amplitudes from the outer shells of heavy atoms as it consumes large amounts of computer time. Moreover, at higher photon energies the accuracy of the codes is found to deteriorate. The modified form factor (MFF) approximation is used for estimating outer electron Rayleigh amplitudes of heavy atoms in which $T >> m$. Franz had defined the modified form factor $g_i(\Delta)$ as

$$g_i(\Delta) = 4\pi \int_0^\infty \rho_i(r) \frac{\sin(\Delta r)}{(\Delta r)} \left[\frac{mc^2}{E_i - V(r)} \right] r^2 dr \qquad (1.31)$$

Where ρ_i is the charge distribution, E_i the total energy of the ith electron, and $V(r)$ is the potential energy of a charge e at position $\vec{r}$ due to the nucleus and the other atomic

electrons. The issues related to the validity of form factors in different approximations can be found in [70]

Kissel and Pratt [56] have prescribed S-matrix method for inner shell amplitudes and the following equations for estimating outer electron R-amplitudes corresponding to the i^{th} subshell:

$$\mathrm{Re}\,A_{\perp}^{i} = -r_e g_i(\Delta), \qquad \mathrm{Re}\,A_{\parallel}^{i} = -r_e g_i(\Delta)Cos\theta,$$

$$\mathrm{Im}\,A_{\perp}^{i} = \frac{\sigma_i^{PE}}{\sigma_{inner}^{PE}}[\mathrm{Im}\,A_{\perp}^{inner}], \qquad \mathrm{Im}\,A_{\parallel}^{i} = \frac{\sigma_i^{PE}}{\sigma_{inner}^{PE}}[\mathrm{Im}\,A_{\parallel}^{inner}], \tag{1.32}$$

where σ^{PE} is the photoelectric cross section. Following this approach, Kane *et al.* [67] have tabulated elastic cross section of selected elements for low energy γ-ray (0.0595-1.332 MeV).

The S-matrix method is found to yield poor predictions for low-Z elements [71]. A so called "composite" approach [72] of finding Rayleigh amplitudes involving non-local exchange and electron-correlations correction to the S-matrix method has been suggested. Agreement between the measurements [71,73] and the predictions of the composite method is fairly good.

A database on Rayleigh scattering of low energy γ-ray is also available [74]. For review works on Rayleigh scattering one can refer [56, 67,143].

1.3.2. Nuclear Thomson Scattering

The nuclear Thomson scattering is elastic scattering of photons by nuclear charge distribution. This phenomenon is relatively simple and its amplitudes are well known. Treating the nucleus as a single point-like free particle of charge Ze and mass M, we may write the Thomson scattering amplitude as

$$A_{\perp}^{T} = \frac{-Z^2 m}{M} r_o, \qquad A_{\parallel}^{T} = A_{\perp}^{T} Cos\theta. \tag{1.33}$$

1.3.3. Nuclear Resonance Scattering

In the energy region between 5 and 30 MeV, the resonances in nuclear photo absorption (giant dipole resonance (GDR) region) becomes important and the corresponding scattering process become visible. A semi-empirical expression for nuclear resonances scattering amplitudes can be given by superposition of "Lorentzian lines" [75,76]

$$A_{\perp}^{N} = \frac{E^2}{4\pi\hbar c}\sum_{\nu=1}^{2}\sigma_{\nu}\Gamma_{\nu}\frac{\left(E_{\nu}{}^{2}-E^{2}\right)+iE\Gamma_{\nu}}{\left(E_{\nu}{}^{2}-E^{2}\right)^{2}+E_{\nu}{}^{2}\Gamma_{\nu}{}^{2}},$$

$$A_{\parallel}^{N} = A_{\perp}^{N}Cos\theta \qquad (1.34)$$

where ν = 1 for spherical nuclei and 2 for deformed nuclei. In eqn. (1.34) the GDR parameters σ_{ν}, width Γ_{ν} and resonance energy E_{ν} are determined by experiments.

1.4. Experimental Investigation

1.4.1. Introduction

The contribution of four elastic scattering amplitudes, namely, A^R, A^T A^N, and A^D to the total differential elastic scattering cross-section varies with photon energy (ω), atomic number (Z) of the scatterer, and scattering angle (θ). The four different elastic processes cannot be distinguished experimentally. In a scattering experiment one essentially measures the total number of scattered photon of particular energy within a solid angle per unit of time for an incident flux of mono-energetic radiation from which one estimates $d\sigma/d\Omega$, the elastic differential scattering cross-section. So, in principle, experimental investigation of any one of these four processes is possible if the other three

processes are accurately known. In spite of this difficulty, knowledge about the general behavior of the four amplitudes can provide "window" to an experimentalist. Let us mention some of these properties here. A^R dominates for $\omega \leq 1$ MeV, most angles and heavy nuclei. For energies $\omega \geq 6$ MeV and $\theta \geq 20^o$ the amplitude A^R is negligible. A^T is well known and becomes important at $\omega \approx 1$ MeV, $\theta > 60^o$ and light elements. In the energy region between 5 MeV and 30 MeV, A^D and A^N are of comparable magnitudes. Outside this region A^N can be neglected. For $\omega > 100$ MeV, $A \approx A^D$.

The selection of ω, Z and θ for an experimental observation of elastic photon-atom processes is guided by, beside the main motivation of the experiment, the general behavior of elastic amplitudes. For example, low-energy photons (few MeV) are used to investigate the real part of Delbrück scattering whereas high-energy photons are suitable for its imaginary part.

The content of this section is as follows. Through *Sec.* 1.4.1.1 to 1.4.1.3 a concise description of detectors, sources and scatterers used in different experiments have been outlined. In *Sec.* 1.4.2 important experiments and their results are presented.

1.4.1.1. Detectors

Different generations of detectors, ranging from G.M. counter [2] to the latest high purity semiconductor detectors, have been used in the long pursuit of the study of Delbrück scattering. The efficiency and energy resolution are the basic concerns of a detector. An ideal detector should not only detect scattered photons but it must also have sufficient energy resolution so that an elastically scattered photon is distinct from inelastically scattered ones.

NaI (Tl) detector is characterized by relatively better efficiency (for example the photopeak detection efficiency of a 5 cm. diameter cylindrical NaI (Tl) detector of 5 cm. height is about 10 % at 1.332 MeV) but poor energy resolution (full width at half maximum increases to 75 keV at 1.332 MeV from 5 keV at 14.4 keV). High resolution semiconductor detectors such as Ge (Li) became commercially available since 1960s.

Large volume high purity germanium (HPGe) detector (Resolution: about 2 keV at 1.33 MeV) are in use since 1980s. Because of low atomic numbers (Z=14 for Si and Z=32 for Ge) the detection efficiency of semiconductor detectors diminishes with increasing photon energy. As such, NaI (Tl) detectors are still in use at energies of the order of 20 MeV. The Si (Li) detector is preferred over germanium detectors at X-ray energy regime [77]. HPGe detector need not be kept at liquid nitrogen temperature throughout as in the case of lithium drifted detectors. However, during an experiment, HPGe detector must be operated at liquid nitrogen temperature.

In most of the semiconductor detectors operating at liquid nitrogen temperature, preamplifier is incorporated as part of the cryostat package to achieve minimum electronic noise. The design of preamplifiers is constrained by two conflicting criteria: (1) low-noise output ;(2) high counting rate capability. The output signals coming from preamplifier have to be amplified, shaped suitably and then processed with the help of a multichannel pulse height analyzer. The full width at half maximum $(\Delta E_{photopeak})^2$ of the detector photopeak can be written as

$$(\Delta E_{photopeak})^2 = (\Delta E_D)^2 + (\Delta E_X)^2 + (\Delta E_E)^2 \qquad (1.35)$$

The first term of the right-hand side, $(\Delta E_D)^2$ represents inherent statistical fluctuation in the number of charge carriers created and is given by $(\Delta E_D)^2 = (2.35)^2 F \varepsilon \omega$ where F is the Fano factor, ε is the energy necessary to create one electron-hole pair, and ω is the photon energy. The second term $(\Delta E_X)^2$ arises due to incomplete charge collection and is most significant in detectors of large volume and low average electric field. Ideally, charge collection would be complete if the field is infinite. Its magnitude can be estimated experimentally by carrying out a series of FWHM measurements as the applied voltage is varied. The third factor $(\Delta E_E)^2$ represents the broadening effects of all electronic components following the detector. This can also be estimated by a simple experiment [77].The spectroscopic amplifier not only amplifies the preamplifier output, but also acts as a signal processor. The inbuilt differentiator acts as a base-line restorer, clipping slow or defective pulses. Precise trailing edge cancellation is ensured by a

pole/zero adjustment. The stability of the gain of the amplifiers becomes important for high resolution experiment and low event-rate scattering processes.

The high-energy small-angle measurements have been done with different arrangements for detecting scattered photons. For example, a Cerenkov counter of a single crystal of thallous chloride coupled with a photomultiplier tube [78], magnetic pair spectrometer [79], electromagnetic calorimeter based on liquid krypton [11] etc. have been used.

1.4.1.2. Sources

Sources such as radioactive isotopes, bremsstrahlung beams from electron accelerators with filtering and/or tagging facilities, radiation from electron synchrotrons, γ–rays produced from in-beam (n, γ) reactions etc. have been used. Reactor or accelerator produced radioisotopes are the usual source for energies up to the order of few MeV. Fission products, such as ^{137}Cs (661.6 keV), are also used as sources. The γ-rays of 4.3-11.4 MeV energy produced by (n, γ) reactions have been used in the study of Delbrück scattering [80]. Bremsstrahlung radiation having energies between 1 to 7 GeV was produced at DESY (Hamburg) electron synchrotron [79]. Bremsstrahlung radiation sources are found to possess spread in energy [81]. With the development of tagged photon beams, the energy spread has been reduced [82]. Use of monochromator [83] further reduces the spread. The γ-rays in the energy range from 20 to 100 MeV were produced using tagged photon technique [78]. High energy photons produced via backward Compton scattering of low energy laser photons by high energy electrons have been used in [11].

1.4.1.3. Scatterers

Most of the experiments involving Delbrück scattering is carried out with solid scatterer. Choice of a target is subjected to two conflicting requirements: (1) to have a

large number of scattering points, in order to get reasonable scattering events; (2) to have very small dimensions so that angular spread, multiple scattering and bremsstrahlung radiation produced by secondary electrons in the target are reduced. Thin scatterers, mostly solids, are used so that $\mu t \langle\langle 1$, where μ is the attenuation coefficient and t is the target thickness. It is suggested [67] that in order to get reasonable counting rates with sources of moderate intensity (~1 Ci), μt may be chosen as large as 0.4. To achieve high counting rates and small angular spread using thin scatterers, targets having the shape of a surface of revolution about the source-detector axis have been used [84-86]. As the cross section for Delbrück scattering goes as $(\alpha Z)^4$, a high Z target is favorable.

1.4.2. Experimental results

In the following sections are presented the results of some important experiments performed so far and their comparison with the relevant theoretical prediction(s) have been made. This section has also been classified into three ranges depending upon photon energy and angle of scattering as in the case of theory part: High energy and small angle, Low energy and all angles, and Intermediate energy and moderately large angles.

1.4.2.1. High-energy small-angle experiments

The high-energy elastic scattering of photons by atoms is largely dominated by the imaginary part of Delbrück scattering amplitude. Such high-energy photons are usually produced by bremsstrahlung in electron synchrotron.

The first definite observation of Delbrück scattering was reported by Jarlskog *et al.* [79] at a precise high-energy experiment. The scattering cross sections of Cu, Ag, Au and U were measured at energies between 1 and 7 GeV and scattering angles between 1 and 3 mrad. A well collimated bremsstrahlung beam from the DESY electron synchrotron was used in the experiment. The incoming photon beam had a bremsstrahlung energy spectrum of maximum values E_0 which could be set at 1, 2, 4, and

7.3 GeV. Scattered photons were detected by a pair spectrometer. Elaborate care was taken to eliminate background. The experimental error at lower Δ (Δ~2MeV/c) was ~8% and it went up to about 20% at Δ =19.6 MeV/c. The findings of [79] were in good agreement with the theoretical prediction of [42] as shown in Fig.1.6. In the earlier experiment [78] at an energy of about 87 MeV and between scattering angles of 1 and 5 mrad the Delbrück effect was clearly detected but the cross section measured in [78] could not be used to discriminate between the predictions by Bethe and Rohrlich [26] and Cheng and Wu [35,36].

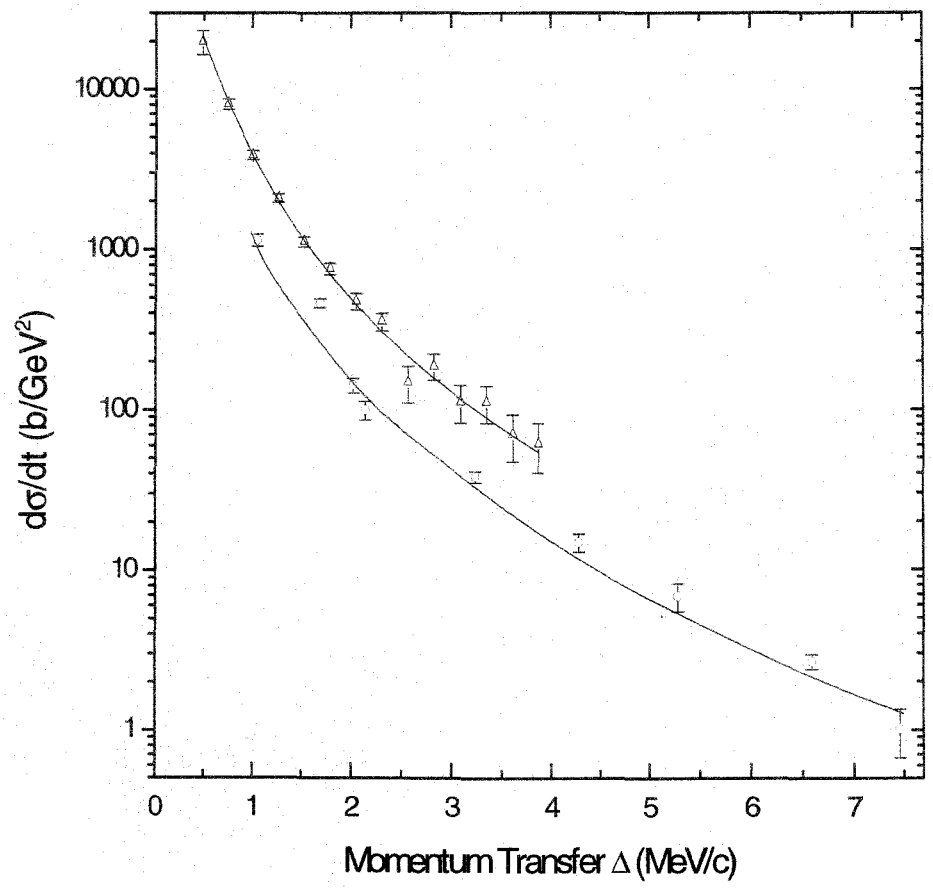

Fig.1.6. High-energy small-angle measurements of Delbrück scattering cross sections. Circles denote cross sections for uranium and triangles denote the same for bismuth germanate ($Bi_4Ge_3O_{12}$). In this figure $d\sigma/dt$ has been plotted against Δ where $d\sigma/dt = (\pi/\omega^2)(d\sigma/d\Omega)$ and $t = \Delta^2$. The solid lines describe the theoretical predictions. The data are taken from [79] and [11].

Few other experiments [87, 88] conducted prior to [79], in the small angle region, had also demonstrated the presence of imaginary Delbrück amplitude.

In a pioneering experiment Akhmadaliev et al [11] measured Delbrück scattering cross sections at photon energies 140-450 MeV and at angles between 2.6 and 16.6 mrad using tagged backscattered Compton photon. They used a detector (electromagnetic calorimeter) having a resolution of $2.4\%\sqrt{E(GeV)}$. The experimental error is found to increase from 6% at Δ =1.01MeV/c to 34% at Δ =3.87 MeV/c. The measurement was in agreement with theoretical predictions of [32, 33] although [42] also yields the same result (see the upper curve of Fig.1.6). They have also reported first experimental observation of photon splitting in [11]. The photon splitting in Coulomb field has also been observed in the above experiment [89].

1.4.2.2. Low energy experiments

From the analyticity properties of the scattering amplitudes, it is well known that the real Delbrück amplitude must be present as a corollary of the imaginary amplitude. For $\omega < 2m$ Delbrück amplitude is purely real and up to a few MeV the real part is significant. Detection of real part posed as an interesting issue and the measurements at energies of a few MeV were performed for many decades.

Before the calculation of real part [28] was published, the discrepancy between the measurements at 2.62 MeV [90] and theoretical prediction excluding Delbrück amplitude was taken as evidence for the existence of Delbrück scattering. Inclusion of Delbrück amplitudes from [28] in the sum of other elastic amplitudes did not remove the discrepancies. Later, Hardie *et al.* [91] pointed out that possible reasons for that discrepancy could have been inaccurate calculations or systematic errors in the experiments or both. The discrepancy, then, could not be taken as an evidence for the existence of Delbrück scattering. Later it was claimed [47, 49] that the dispersion relation used in [28] to calculate the real part at an arbitrary angle was inadequate because of the nature of its singularities.

The early definite evidence for the existence of the real part of the Delbrück amplitude was reported by Schumacher *et al.* [92]. They used 2.754 MeV photons from Na-24 source (prepared by bombarding aluminum with deuterons in the internal beam of Göttingen synchro-cyclotron) and a 76-cm^3 Ge (Li) detector having a resolution of 2.1 keV at 1.33 MeV.

The choice of photon energy in the above experiment was favorable for the detection of the real part of Delbrück scattering amplitude since at 2.754 MeV the real part is larger than the imaginary part and also the contributions of Rayleigh and Nuclear resonance scattering to the elastic scattering are negligibly small.

At large scattering angles the number of elastic-events is less and at intermediate angles the dependence of cross section with angle is more. In accordance with these facts they made experimental set-ups so that (1) at large angles (θ=75-120^0) they minimized background by means of heavy shielding and (2) at intermediate angles they minimized angular spread by optimizing source-target and target-detector distances.

The agreement between the measurements of [92] and the theoretical predictions including Delbrück amplitudes calculated by Papatzacos and Mork [49] and the Rayleigh amplitudes given by Cornille and Chapdelaine [62] was, by and large, good. However, they also noticed that the theoretical predictions were somewhat smaller than the experimental values in the whole angular range from 30° to 90° as shown in the lowermost curve of Fig.1.7 and this difference went up to a factor 1.7 [93]. This departure of the measurements with the theoretical prediction based on the lowest-order Born-approximation Delbrück amplitudes of [49] was thought to be due the non-inclusion of higher-order Feynman diagrams (Coulomb corrections). The contributions from higher order diagrams, particularly for high-Z scatterers, may not be negligible (See *Sec.* 1.4.2.2.1 for Coulomb correction).

The findings of other experiments using Ge (Li) detector, performed before the Göttingen group experiment [92], at energies around 1 MeV [91,94,95] were inconclusive as far as Delbrück scattering part is concerned. For some time there

appeared to be a substantial discrepancy between theory and the experiments for high-Z elements at this energy range.

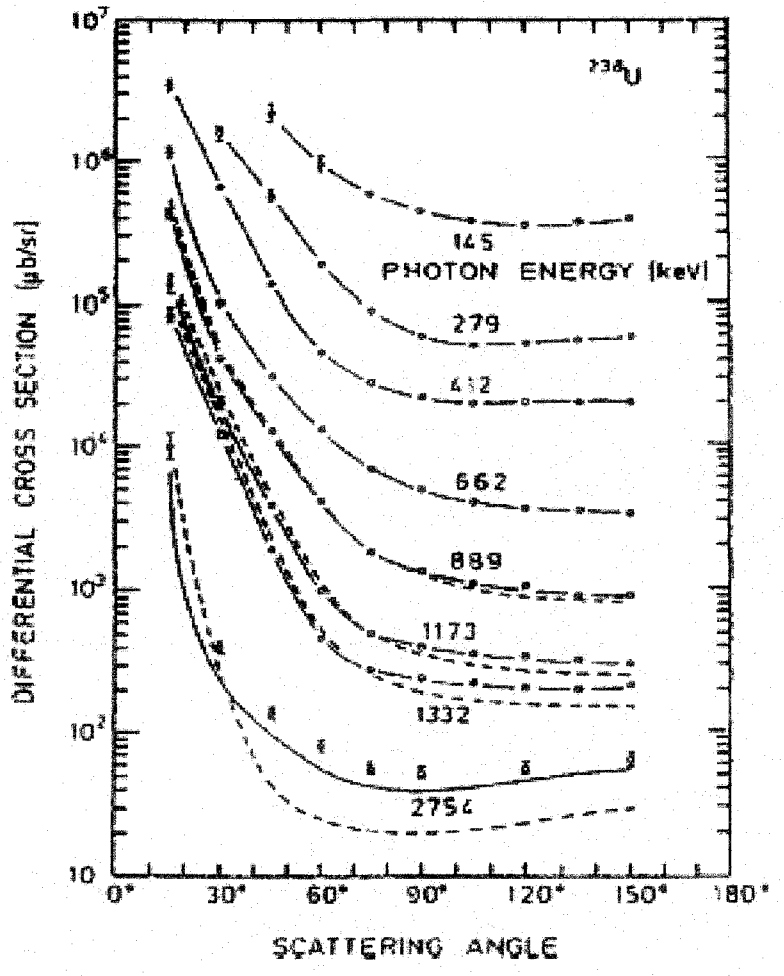

Fig.1.7. Elastic differential cross sections at different photon energies for uranium (Z=92) targets. The solid lines include R, T, N and lowest order D-amplitude; the dashed lines are without D-amplitudes [10].

After the availability of S-matrix Rayleigh amplitudes calculated by Kissel and Pratt [65] most of the discrepancies between theory and the experiments for high-Z elements in the MeV range disappeared. Using the predictions of [65] for Rayleigh amplitudes and that of [49] for Delbrück amplitudes, Basavaraju *et al.* [95] and

Muckenheim and Schumacher [96] clearly found the evidence of real part of Delbrück amplitudes at 1.17 and 1.33 MeV at high-Z. In [95], the elastic scattering cross sections of lead, tantalum and molybdenum for angles between 30^0 and 115^0 were measured using a Ge (Li) detector having active volume 10 cm^3 and resolution of about 5 keV at 1.33 MeV. In [96], a Ge (Li) detector of active volume75 cm^3 and having resolution of about 2 keV at 1.33 MeV, were used to measure the cross sections of uranium at energies between 0.1 and 1.5 MeV in which Delbrück scattering have been observed at energies as low as 0.889 MeV, that is well below pair production threshold (see Fig.1.7).The experimental error in these measurements was 6 to 10 % at 15^o and about 3% at 120^o. The agreement between experiment and theoretical prediction based on S-matrix Rayleigh amplitudes is within 3% [96].

In [66] it has been shown that there were a factor of two errors at back angles in the widely used Rayleigh amplitudes calculation for the K-shell of mercury at energy of 2.56 mc^2 given by Brown *et al.* [61], and this important observation removed the discrepancy between theory and the experiments. It is now well known that the old measurements done by Dixon and Story [94] and Hardie et al. [91, 97] and even older results obtained by Standing and Jovanovich [98] and Basavaraju *et al.* [99] using NaI detector are in good agreements with the theoretical prediction [67]. This implies that these early experiments were sufficiently accurate but their evidence for Delbrück-part was clouded by the inaccurate prediction of Rayleigh amplitudes.

In the energy range between 4 and 12 MeV the Nuclear Resonance Fluorescence due to the excitation of individual nuclear levels is found to compete with other coherent elastic scattering processes making it difficult [100-102] to study Delbrück scattering in the nuclei with low density of nuclear states. At energies between 8.5 and 11.4 MeV, it is found that not only Coulomb corrections to the lowest-order Delbrück amplitudes are needed but also the corrections to the scaling factor for the giant dipole resonance photoabsorption cross sections are necessary [103]. The dominance of nuclear resonance contribution at the above energy ranges were reported in [104, 105].

1.4.2.2.1. Coulomb correction

In the lowest-order Born approximation calculation of Delbrück amplitudes, the contributions of the higher ordered Feynman diagrams (six-cornered loops and beyond in Fig.1.1) are neglected owing to mathematical complexity. Making a Coulomb correction to the lowest-order Born approximation calculation is quantitatively equivalent to the inclusion of higher loops in calculation the Delbrück amplitudes. But, owing to the unavailability of such higher-order calculations, the Coulomb corrections are usually estimated from the experimental data using certain ansatz.

As mentioned earlier the observation at 2.754 MeV [93] that the theoretical prediction based on the lowest-order Born approximation was smaller than the experimental values up to a factor 1.7 was an indication towards the need for Coulomb correction. The investigation of Coulomb effect at 2.754 MeV was carried out extensively by Rullhusen *et al.* [103, 106-110], Schumacher *et al.* [93,111], Schumacher

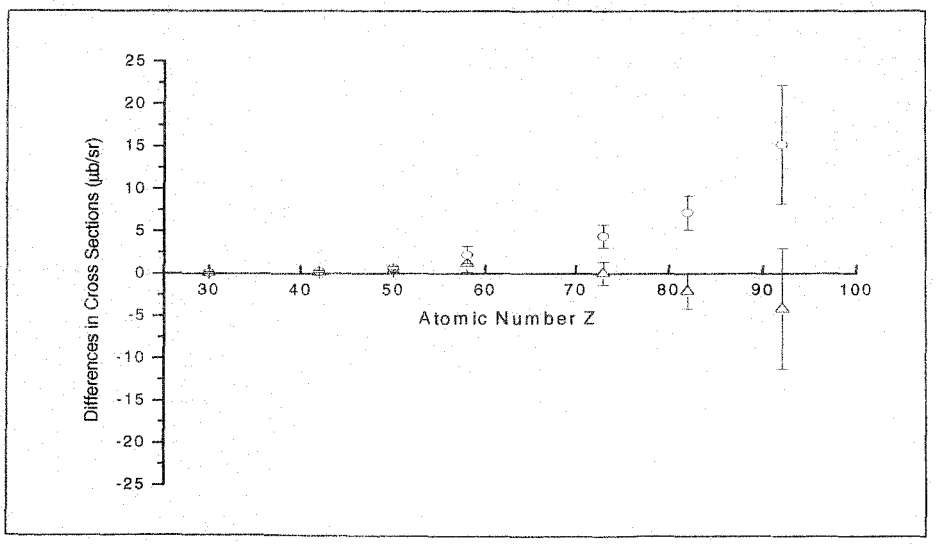

Fig.1.8. The differences between the experimental and theoretical cross sections including Coulomb corrected lowest-order D amplitudes for $\theta = 60^0$ and E=2.754 MeV are represented by triangular points. The circular points represent the similar differences without including Coulomb corrections in theoretical predictions. The experimental results are from [109,113].

and Rullhusen [112], and Kasten *et.al.* [113]. At 2.754 MeV and higher energies, modification of lowest-order Born-approximation Delbrück amplitudes due to Coulomb correction have been found to be large [108]. Due to unavailability of Coulomb correction predictions they tried to identify its effect by measuring Z dependence of the differential cross section. It was found that the Coulomb correction term being of the order of $\alpha(Z\alpha)^4$ is sufficient [111]. Estimation of Coulomb corrections has been done by using the ansatz $A^{cc} = (Z\alpha)^4 g(E) f(\theta)$ [103] where a good fit of experimental data was obtained by taking the function $g(E) = 15.17MeV^{-1} - 0.11MeV^{-3}(E + 6.0MeV)^2$. The predictions including the Coulomb corrected terms obtained via the above procedure were found to match well, within the error limits, with the experimental results whereas the lowest order predictions without including Coulomb corrections deviate, distinctly, away from measured values as illustrated in Fig.1.8.

The validity of Coulomb correction effect of the order $\alpha(Z\alpha)^4$ at different angles and for different Z have been shown in Fig.1.9. At 9 MeV it was found [103] that for Z between 73 and 92 the discrepancy between the lowest-order Born-approximation predictions and the experiments could be removed by empirically introducing a set of additional amplitudes with a common factor of the order $\alpha(Z\alpha)^4$ but there exist interfering components from the giant dipole excitation of the nucleus. Using general properties of scattering amplitudes, tentative estimates of Coulomb correction terms for energies 1-4 MeV were made [113] and the curve so generated matched well with the experimental result for U=92 and E=2.754 MeV as shown in Fig.1.9.

At medium and large angles and with targets of $Z \leq 50$, A^T and A^D are larger than A^R and A^N and the imaginary A^D are smaller than its real part, the Coulomb corrections are small and therefore, the predicted lowest-order Born approximation amplitudes have been found to be sufficient [109] within 5%.

Experiments at energies close to the pair-production threshold were performed with two motives: (1) whether Delbrück scattering is visible, and (2) if so, whether Coulomb correction is needed. At these energies Delbrück scattering have been clearly

observed and these results [15, 95, 96, 114] also show that the lowest-order Born approximation amplitudes are sufficient.

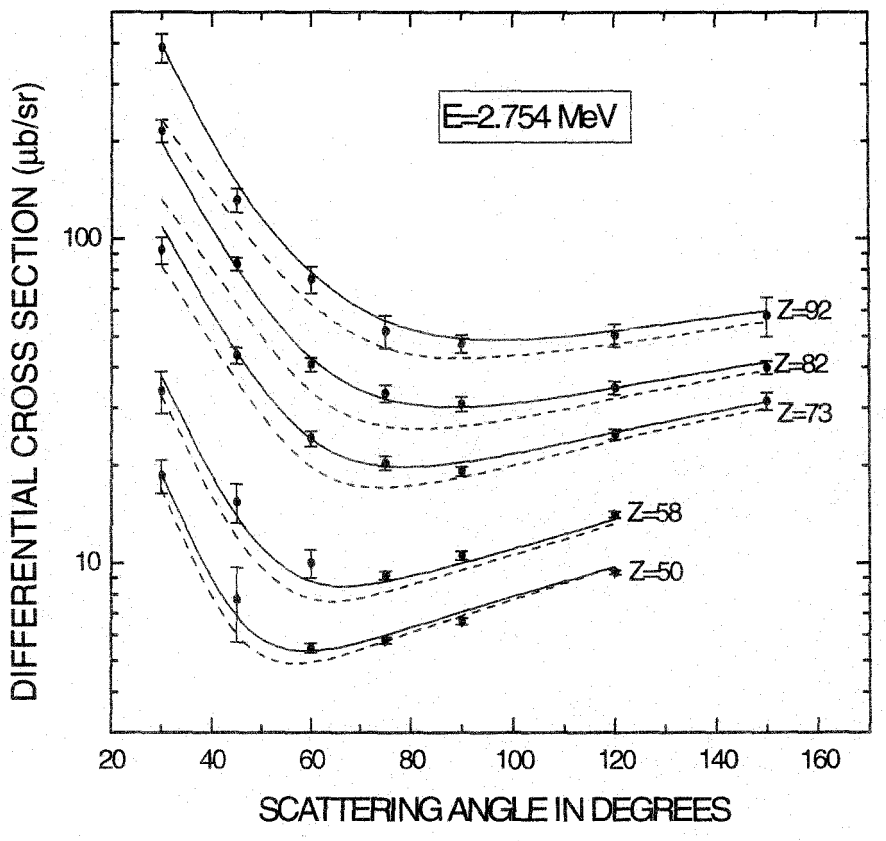

Fig.1.9. Experimental elastic differential scattering cross section for Z=50 to Z=92 and E=2.754 MeV compared with theoretical predictions. The dash- line for each Z include R, N, T, lowest-order D scattering and whereas the solid-line is same as the dash-line but includes also the Coulomb correction effect. Experimental data are taken from [113].

1.4.2.3. Intermediate energy experiments

An experiment, in the energy range between 25 and 100 MeV and at moderately large angles, using Bremsstrahlung tagged quasi-monochromatic photons has been carried out at MAMI A (Germany) [46, 115, 116]. The experimental data is compared

with lowest-order Born-approximation calculation and small-angle high-energy predictions as shown in Fig.1.10. The disagreement between the theoretical and experimental results is not unexpected as the lowest-order Born-approximation calculation and the small-angle high-energy approximation for prediction of Delbrück amplitudes are not valid at higher energies (contribution from Coulomb corrections becomes important) and large angles respectively. The prediction of the large-angle high-energy approximation based on the calculation [45, 46, 54] has also been compared with the experimental data in Fig.1.10 and the agreement between the theory and experiment is not satisfactory as may be noticed from the figure. However, a definite conclusion on the stated mismatch could not be ascertained owing to limited quality of the data (experimental error ~ 30 %). At 20° the theoretical prediction of the large-angle high-energy approximation suggests better agreement with experimental data [116].

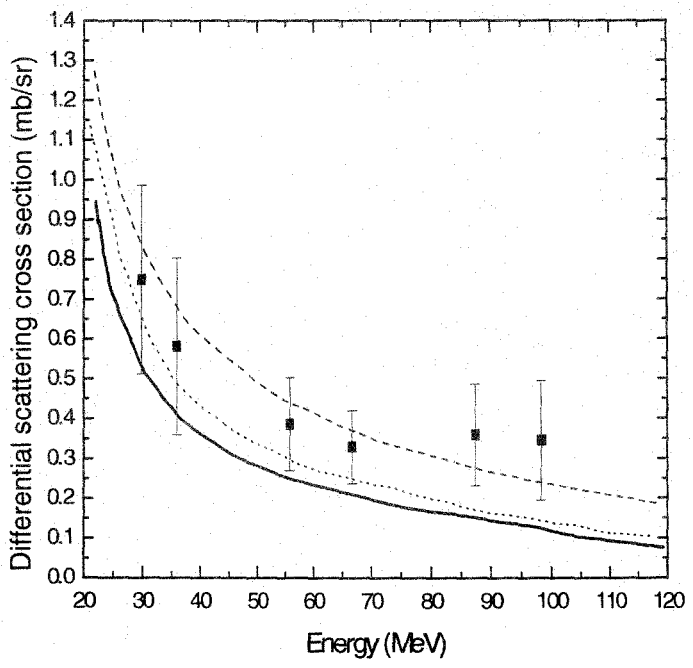

Fig.1.10. Comparison of experimental differential scattering cross section at $\theta = 15^0$ (Z=82) [116] with predictions. Solid curve: including Delbrück scattering calculated in large-angle high-energy approximation [46]; dashed curve: calculating Delbrück scattering in the lowest-order Born approximation; dotted curve [49]: calculating Delbrück scattering in the high-energy small-angle approximation [42].

The presence of Delbrück scattering is, however, clearly established in this energy range irrespective of the large errors in the data. At these energies the elastic scattering from nucleus is very sensitive to electromagnetic polarizability of the bound nucleon and as such it makes the theoretical prediction of elastic scattering more complicated. In other words, comparison of theoretically predicted Delbrück amplitudes with the experimental results could not yield definite conclusion in this range as yet. A better understanding of all the important interfering effects leading to total elastic scattering is needed. At the same time improved experiments are needed to examine the theoretical predictions properly.

1.5. Discussion

Experimentally, Delbrück scattering has been investigated covering a wide range of gamma-ray energies (1-1000 MeV) over the last eight decades. Both, the real as well as the imaginary parts of Delbrück amplitudes have been experimentally detected. On the theoretical side, even though a reasonable understanding of the Delbrück scattering has been achieved so far, there is still no general solution of Delbrück scattering problem for arbitrary photon-energies and scattering-angles. All the theories developed so far have their own ranges of validity. Of these, the theories which are reasonably established include the results for forward scattering [30] and the high-energy small-angle ($\omega >> m, \Delta << \omega$) regime [32, 33, 41, 42].

The calculations of Delbrück amplitude based on the lowest-order Born approximation [49] are found to be valid at lower energies ($\omega \leq 1.33$ MeV) and all scattering angles [15,157]. For larger photon energies ($\omega > 1.33$ MeV), Coulomb correction terms are to be added to the Born approximation amplitudes [103,113]. Thus a general theoretical prediction of Coulomb correction terms are needed until a more general treatment of Delbrück scattering problem valid in this energy regime becomes available.

In spite of all these difficulties the scattering phenomenon has been intensely studied both theoretically and experimentally as it offers, besides its applications in other fields, an attractive opportunity to test the non-linear and non-perturbative regime of quantum electrodynamics.

The Nuclear Resonance Fluorescence due to the excitation of individual nuclear levels, in the energy range between 5 and 15 MeV, is found to compete with other coherent elastic scattering processes. As the contribution of nuclear resonance scattering to the elastic scattering in this energy range is significant, its accurate calculation is possible provided the GDR parameters are precisely determined. A fine tuning of GDR parameters and Coulomb correction estimates can be achieved by means of future experiments in energy range of 5-40 MeV [110].

In the energy range between 20 and 100 MeV, the present experimental results suffer from large uncertainties and thus the predictions of the large-angle high-energy approximation [45, 46, 54] could not be verified at the desired level. Experiments with better accuracies are needed at this energy range for proper testing of the theoretical predictions. The study of elastic scattering in this energy range is of great interest in connection to the question of equality of electromagnetic polarizability of nucleons in free space and in nuclear matter [10].

It is worth mentioning here that in recent years some new possibilities of measuring Delbrück effect have been emerging, such as Delbrück scattering in a Coulomb field in the presence of an external electromagnetic field. Quantum electrodynamics in strong external field is a topic of considerable interest as such a situation is supposed to exist in reality on pulsar atmosphere as well as near the surface of heavy nuclei. In the laboratory a similar situation may be created with the application of intense laser field [12]. Another interesting possibility is the photon emission in collisions of ultra-relativistic heavy nuclei ($Z_1Z_2 \rightarrow Z_1Z_2\,\gamma$) via the virtual Delbrück scattering sub-process [16,17]. The total contribution of virtual Delbrück scattering to the cross section of the photon emission process could be considerably larger than those for ordinary tree-level nuclear bremsstrahlung in the considered photon energy range $m < \omega < m\gamma$, where γ is the Lorentz factor of the nucleus [17]. This provides an attractive opening to

investigate the phenomenon experimentally at a future/ongoing ultra-relativistic heavy nuclei collision experiment such as the RHIC collider or the LHC collider.